Journal of Applied Polymer Science

Ageing properties of polyurethane methacrylate and off-stoichiometry thiol-ene polymers after nitrogen and argon plasma treatment

Tiam Foo Chen,[1] Kim Shyong Siow,[1] Pei Yuen Ng,[2] Mui Hoon Nai,[3] Chwee Teck Lim,[3,4] Burhanuddin Yeop Majlis[1]

[1]Institute of Microengineering and Nanoelectronics, Universiti Kebangsaan Malaysia, Bangi, Selangor 43600, Malaysia
[2]Faculty of Pharmacy, Universiti Kebangsaan Malaysia, Kuala Lumpur 50300, Malaysia
[3]Mechanobiology Institute, National University of Singapore, 5A Engineering Drive 1, Singapore 117411, Singapore
[4]Department of Biomedical Engineering, National University of Singapore, 9 Engineering Drive 1, Singapore 117575, Singapore
Correspondence to: K. S. Siow (E-mail: kimsiow@ukm.edu.my or kimshyong@gmail.com)

ABSTRACT: Proprietary mixture of polyurethane methacrylate (PUMA) and off-stoichiometry thiol-ene (OSTE-80) are evaluated as two possible polymeric substrates to prototype microfluidic biochips. Because of their lack of biocompatibility, PUMA and OSTE-80 are modified by argon (Ar) or nitrogen (N_2) plasma treatment to introduce nitrogen moieties that are highly polar and conducive for cell attachment and growth. XPS and water contact angle measurement show that these nitrogen groups are relatively stable in the plasma-treated PUMA and OSTE-80 in spite of the hydrophobic recovery and volatilization of nitrogen moieties during air ageing for 15 days. This stability can be attributed to their high degree crosslinking that is reflected by the increase of elastic modulus of PUMA and OSTE-80 during their air ageing. These results show that Ar and N_2 plasma-treated PUMA and OSTE-80 possess the necessary physical and chemical properties to be evaluated further to develop microfluidic biochips for biological applications. © 2016 Wiley Periodicals, Inc. J. Appl. Polym. Sci. **2016**, *133*, 44107.

KEYWORDS: ageing; crosslinking; microfluidics; properties and characterization; surfaces and interfaces

Received 9 April 2016; accepted 25 June 2016
DOI: 10.1002/app.44107

INTRODUCTION

Polymers are widely used in the development of microfluidic devices. Compared to glass and silicon-based materials, polymer has several advantages such as low cost, high transparency, and ease of fabrication. The most widely researched polymer for such applications is polydimethylsiloxane (PDMS) which are typically used to prototype lab-on-chip via the soft lithography technique. Some targeted applications of this biochip included membrane dialysis application, renal cell analysis,[1] and cancer cell separation.[2] However, PDMS suffered from several limitations such as adsorption of hydrophobic molecules when submerged in the biological environment,[3] leaching of uncross-linked oligomers from PDMS,[3,4] and low Young's modulus for certain lab-on-chip applications.[5,6] Surface modification techniques were used to address these shortcomings but unable to meet all requirements for the intended applications because of the surface hydrophobic recovery on the surface-modified PDMS.[7]

Besides PDMS, polyurethane methacrylate (PUMA) were also explored as a potential prototyping polymer for microfluidic devices. One such PUMA-based device consists of microstructures or micro-pillars of high-aspect-ratio formed via a simple UV-casting procedure.[8] According to Kuo *et al.*, the native PUMA (Dymax 140-M, USA) possessed stable electro-osmotic flow properties when stored up to 12 days in ambient conditions.[9] Another variant of PUMA, Polydiam SF-45 Photopolymer (UK), also possessed other suitable properties such as high chemical and thermal stability, high optical transparency, and strong interfacial bonding strength to form the microfluidic device.[10] The properties of PUMA attracted several process and design innovations to produce lab-on-chip for various applications such as blood cell or cancer cell separation.[8–11]

Besides PDMS and PUMA, another polymer known as off-stoichiometry thiol-ene (OSTE) has also shown potential to be a prototyping material for the microfluidic devices. OSTE had unreacted side groups, i.e., either thiol or ene functional group on the surface, and these unreacted groups allowed OSTE polymer to be modified through the "Click" reaction for subsequent covalent bonding of microfluidic devices.[12,13] The one-step

Additional Supporting Information may be found in the online version of this article.

bonding of OSTE is an advantage in reducing process steps and increasing reliability over the additional thermal bonding employed by other polymeric materials used in microfluidic devices. In addition, the mechanical properties of OSTE can be designed by the ratio of the two components of off-stoichiometry prepolymers to meet the structural integrity of the microfluidic devices or the softer pumps, mixers, and valves in these devices.[6]

In spite of their favorable mechanical, thermal, and chemical properties, PUMA and OSTE lack the biocompatible properties required in the cell-based microfluidic devices. Cells cultured on the OSTE-based microfluidic devices showed low viability.[14] Similarly, PUMA also showed unsatisfactory result when used in micro-filter to isolate the blood cells.[8] Therefore, the surface properties of PUMA and OSTE need to be modified while maintaining their mechanical and thermal properties. Plasma-modification is one possible approach because of its track record in surface modifications for biocompatibility and cell-interactions.[15,16]

The plasma-based modification is divided into plasma polymerization and plasma treatment. Plasma polymerization deposits nanometer thickness of reactive moieties while plasma treatment inserts similar reactive moieties on the polymer surfaces without modifying the bulk properties of the polymer. Here, we used the plasma treatment approach, i.e., an inert argon (Ar) and a reactive nitrogen (N_2) gas plasma treatment to modify PUMA and OSTE to achieve the desired physical-chemical properties. Nitrogen plasma treatment introduces nitrogen and oxygen moieties which increase the surface energy of the polymers and enhance their biocompatibility with cells.[17] Ar plasma treatment creates free radicals in the polymer which subsequently cross-linked amongst themselves or oxidizes to peroxide for grafting with other reactive biomolecules.[15] Besides the usual carboxyl and hydroxyl functionalities from the oxidized carbon group, Ar plasma treatment also introduced nitrogen moieties on to the polymeric substrate at high plasma discharge power.[18] While these mentioned plasma-induced changes were successfully demonstrated for various polymers,[19–22] similar work had not been investigated on PUMA and OSTE polymers.

In this article, we found that the Ar and N_2 plasma treatment produce favorable changes to the proprietary mixture of PUMA and OSTE (known as OSTE-80) polymers in term of surface roughness, Young's modulus, water contact angle/hydrophilicity, and surface chemical functionalities. The plasma-treated PUMA and OSTE-80 also maintained their high densities of nitrogen moieties, which will be essential in mediating the bio-interfacial reactions with cells and biomolecules in our next work in cell and protein interactions.

EXPERIMENTAL

Preparation of PUMA and OSTE-80

Proprietary mixture of PUMA with product code Polydiam SF-45 Photopolymer was procured from Polydiam Industries Limited, United Kingdom. OSTE with the product name of OSTEMER Thiol 80 (hereafter known as OSTE-80) was purchased from Mercene Labs, Sweden. Figure 1 shows the molecular structure of the two main components of OSTE-80 prepolymers. In addition, OSTE-80 prepolymers contained other proprietary UV-initiators and activators.

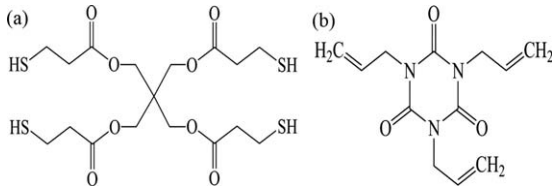

Figure 1. Molecular structures of OSTE-80 prepolymers are: (a) pentaerythrithiol tetrakis (3-mercaptopropionate) (CAS:7575-23-7) and (b) 1,3,5-triallyl-1,3,5-triazine-2,4,6(1H,3H,5H)-trione (CAS:1025-15-6).

Separately, PUMA and OSTE-80 prepolymers were spin-coated on top of a 1 cm^2 of silicon. These deposited prepolymers were then covered with a transparent polyester sheet and cured under UV-light exposure (wavelength: 365 nm; light intensity: ~2.0 mW cm^{-2}) for 15 minutes.[10,23] Next, the UV-cured polymers were washed with copious supply of Milli-Q water (18.2 MΩ cm^{-1} @ 25 °C) and dried with dry nitrogen before Ar and N_2 plasma treatment. The average thickness of the PUMA and OSTE-80 polymers were 100 μm, based on masking and measurements with the surface profiler (brand: Dektak 150, Vecco).

Plasma Treatment

The plasma treatment was carried out in a custom-built reactor discussed elsewhere.[24] The reactor consisted of an upper U-shaped copper electrode and a bottom circular copper electrode. The plasma formed inside the reactor was generated by a radio frequency generator (RF-3-XIII) operating at 13.56 MHz with impedance matching. The UV-cured PUMA and OSTE-80 polymers were placed on the bottom electrode. The pressure of the reactor was pumped down to 1.5 Pa. The precursor, either N_2 or Ar, was then fed into the reactor controlled by a needle valve. The pressure inside the plasma chamber was monitored by a CVM211 stinger vacuum gauge and this pressure was converted to flow rate based on the following equation:

$$F = \frac{dp}{dt} \times 16172 \frac{V}{T} \quad (1)$$

where p is the pressure (mbar), t the time (s), V the volume of plasma reactor (12.7 L), and T the temperature (295 K).

The plasma was ignited at 20 watts of discharge power for the PUMA and OSTE-80 polymers when the flow rate reached 10 sccm. The plasma treatment time required for PUMA and OSTE-80 polymers were 60 and 30 seconds, respectively. The plasma-treated PUMA and OSTE-80 polymers were washed with copious supply of Milli-Q water (18.2 MΩ cm^{-1} @ 25 °C) and dried with nitrogen gas before subjected to surface characterization.

Surface Characterization

Fourier Transform Infrared Spectroscopy (FTIR). Fourier transform infrared spectroscopy (FTIR-ATR; Spectrum 400 Perkin Elmer spectroscopy) was used to identify the functional groups on PUMA and OSTE-80 during the stages of prepolymer, polymer and plasma-treated polymers. All infra-red

measurements were obtained through 64 scans with a resolution of 4 cm^{-1} and followed by background subtraction.

Water Contact Angle Measurement (WCA). After Ar or N_2 plasma treatment, the water contact angles (WCA) of PUMA and OSTE-80 polymers were measured by VCA Optima (AST Products,) based on the sessile drop technique at room temperature. Milli-Q water droplets of 2 μL were placed on the sample surface with a micro-syringe. In order to ensure repeatability, the measurements were repeated at three different locations for each sample, and each sample was prepared at least in triplicates ($n = 9$). Plasma-treated samples were aged in the different environment, i.e., ambient air, Milli-Q water, and phosphate buffer solution (PBS) to study their changes in water contact angle. The PBS was prepared by dissolving one tablet (Product No: P4417 Sigma) in 200 mL of Milli-Q water.

Atomic Force Microscopy (AFM). The images of the surface topography, average roughness (Ra), and root mean square roughness (Rq) of the as plasma-treated and untreated substrates were taken using an atomic force microscope (AFM) (Brand: Solver Next, NT-MDT). The samples were scanned using tapping mode in air with the golden silicon probes NSG10 tips. These tips had a typical resonance frequency of 240 kHz and a spring constant of 11.8 N m^{-1}. The scan size of the samples was 25 μm^2 with 256 points per line. Each measurement was repeated thrice.

The elastic moduli of samples were measured by another AFM (Brand: Nanowizard II with JPK proprietary software) with Bruker MSCT tip in PBS mixed with 0.1% bovine serum albumin. The tip has a typical spring constant of 0.72 N m^{-1}. A maximum load of 20 nN was applied for force–displacement curves. Twenty locations per sample were taken for each plasma-treated PUMA and OSTE-80 polymer. The Hertz contact model was used to obtain the elastic modulus of the samples from curve fitting the extended region of the force–displacement curve. The Poisson's ratio of the polymer samples was assumed to be 0.5.[25]

X-ray Photoelectron Spectroscopy (XPS). The effect of the plasma treatment on the surface chemical properties of PUMA and OSTE prepolymers were analyzed by X-ray Photoelectron Spectroscopy (XPS) (Brand: ULVAC-PHI Quantera II) with the monochromatic Al K_α radiation ($h\nu = 1486.6$ eV) operating the power of 25 W. The vacuum maintained at 10^{-9} mbar throughout the XPS analysis. All spectra were collected at a take-off angle of 45° to the sample surface. The survey spectra were taken with a pass energy of 280 and 1.0 eV energy step for five scans. The high-resolution spectra of C1s, N1s, and S2p peaks were acquired for five scans at a pass energy of 112 eV with 0.1 eV energy step. Atomic percentage were calculated from survey spectra with SmartSoft-XPS version 3.5.1.1 (ULVAC-PHI). The high-resolution spectra were component-fitted by CasaXPS version 2.3.16 with a Gaussian–Lorentzian peak shapes of 70% Gaussian and 30% Lorentzian. Shirley's background was subtracted from these high-resolution spectra during component-fitting. The binding energy of the component C—C, C—H for C1s spectra was shifted to 285.0 eV to compensate for the effect of surface-charging during XPS analysis. The full-width half-maximum values were maintained between 1.2 to 1.8 eV during the component fitting of C1s, N1s, and S2p peaks. Since the S2p peak is a doublet, additional criteria for component-fitting the spectra was adopted namely, the peak area under the $S2p_{1/2}$ was 50% of the $S2p_{3/2}$ and the difference in binding energy between these two peaks were set to 1.2 eV.[26] New samples were taken for each XPS analysis and different days of ageing in air to avoid cross-contamination and X-ray induced damages.

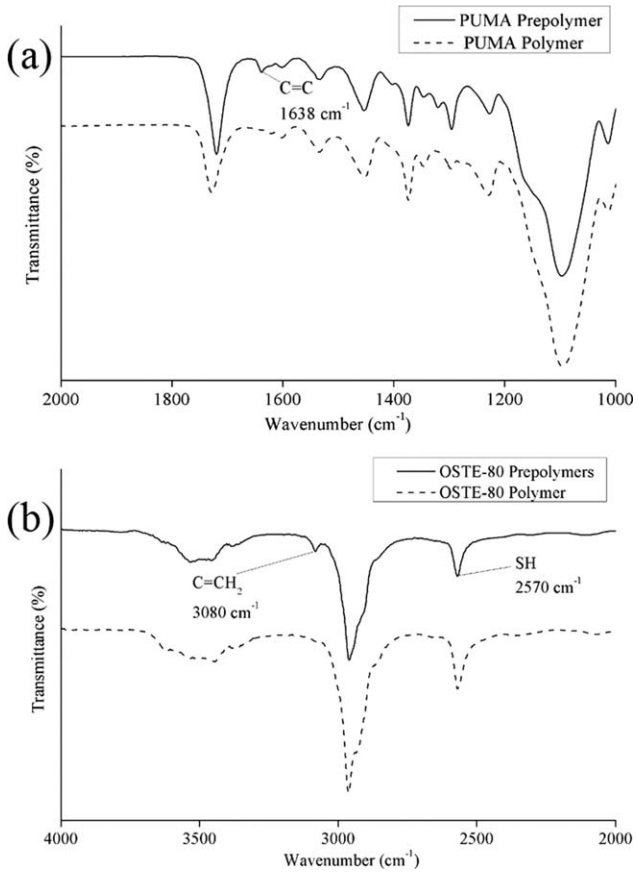

Figure 2. FTIR spectra of the (a) PUMA prepolymer and (b) OSTE prepolymers before and after 15 minutes of UV-curing. Note: IR spectra are offset for clarity.

RESULTS AND DISCUSSION

FTIR Analysis of PUMA and OSTE-80 Prepolymers and Their Polymers

Figure 2(a) compares the FTIR spectra for PUMA prepolymers and PUMA polymer; the C=C bands from the prepolymer disappeared upon UV-curing.[27,28] This C=C bands was likely to be from methacrylate groups of PUMA prepolymer though the actual mechanism was not known because of its proprietary mixture. Similarly, Figure 2(b) shows the disappearance of $C{=}CH_2$ bands for the UV-cured OSTE-80 polymers compared to their prepolymers.[28,29] The $C{=}CH_2$ ene functional groups from the triallyl prepolymers [Figure 1(b)] reacted with thiyl radicals from the thiol prepolymers [Figure 1(a)] until completion because OSTE-80 prepolymers were formulated to have an excess of the thiol prepolymer.[6] This excess thiol groups were later confirmed in the XPS analysis.

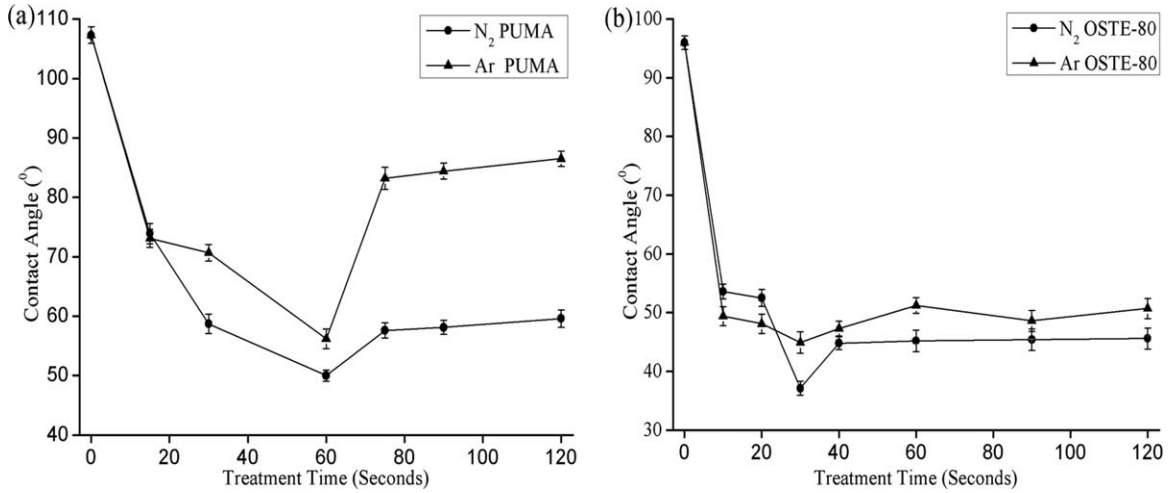

Figure 3. WCA of the (a) PUMA and (b) OSTE-80 polymers after different durations of Ar and N_2 plasma treatment at a flow rate of 10 sccm and discharge power of 20 W. The "0 second" point indicated the WCA of PUMA and OSTE-80 polymers.

However, the FTIR analysis did not show any noticeable differences in their spectra before and after plasma treatment on the OSTE-80 and PUMA polymers (Note: spectra is not included here). The similarities between these infra-red spectra suggested that the plasma treatment only affects the chemical changes at the sub-micron level of the polymers; these sub-micron changes were reflected in the subsequent characterization by WCA and XPS analysis which will be discussed next. Such sub-micron changes reflect the benefits of plasma treatment as compared to the wet-chemistry approach which typically modifies the entire bulk polymer as well as the surface properties.

Plasma-treated PUMA and OSTE-80 Polymers

WCA and Surface Roughness. It is important to measure the WCA and related surface roughness of the plasma-treated substrates because the plasma ions etching and their corresponding changes affect the biological responses in the biochip besides the notable changes in chemical properties. Typically, Ar and N_2 plasma treatments produce hydrophilic surfaces and reduce WCAs but prolonged treatment can roughen and increase the WCAs.

Figure 3(a,b) show the changes in WCA for the PUMA and OSTE-80 polymers after different durations for Ar and N_2 plasma treatment. Despite different precursors for the plasma treatment, PUMA and OSTE-80 polymers showed the lowest WCA after 60 and 30 seconds of plasma treatments, respectively. The reduction in WCA could be attributed to changes in chemical properties and surface roughness induced by the Ar and N_2 plasma treatment. The chemical changes will be elucidated in the XPS analysis discussed in XPS Analysis Section. In short, N_2 and Ar plasma treatment and their subsequent postplasma oxidation introduced various polar groups like carboxyl, amine, and hydroxyl onto the hydrophobic PUMA and OSTE-80 polymers, and such moieties rendered the substrates to be hydrophilic.

Based on Figure 3(a), the WCA increased after 60 seconds of N_2 or Ar plasma treatment on the PUMA polymers because of further etching and ablation of the polar groups and increase in roughness.[20] Unlike PUMA polymer, OSTE-80 polymer maintained these low WCA beyond 30 seconds of Ar or N_2 plasma treatment. These differences were likely to be attributed to the different polymeric morphology and structures of PUMA and OSTE-80 under the ion bombardments during the Ar or N_2 plasma treatment.

Figure 4 shows that PUMA has a rougher surface than OSTE-80 polymer after Ar or N_2 plasma treatment. (Note: The AFM surface topography for all polymers is provided in the Supporting Information.) In addition, PUMA polymer roughened 20–35 times of the untreated polymer, while the OSTE-80 polymer smoothened during the Ar or N_2 plasma treatment. PUMA polymers consisted of soft and hard segments which have different sensitivities to the plasma ablation.[30] The preferential etching of the soft segments in PUMA polymer resulted in an increase of roughness after Ar or N_2 plasma treatment though N_2 plasma resulted in higher Ra and Rq than those treated by Ar plasma treatment. A similar result has been reported by others; the Ra of N_2 plasma-treated cyclic olefin copolymer or PET were higher than those plasma-treated by Ar plasma.[21,31]

On the other hand, OSTE-80 polymer consisted of homogeneous amorphous phase which smoothened after plasma treatment though the absolute reduction was less than 1 nm. Similar results on polymers of different crystallinity have been reported by others; plasma-treated amorphous polymer produced a smoother surface than the polymer with higher crystallinity.[32] Unlike PUMA polymer, the change in water contact angle for OSTE-80 polymer could only be attributed to the chemical changes which will be discussed next.

In spite of different plasma treatment, the resulting surface roughness PUMA and OSTE-80 polymers were not expected to pose any physical hindrance during cell adhesion studies because of their small average roughness of less than 100 nm.[33]

XPS Analysis. ***Ar and N_2 plasma treatment on PUMA polymer.*** Based on Table I, the XPS analysis did not show any nitrogen atoms on the PUMA polymer though the urethane groups of PUMA possess nitrogen as part of the amide bonds. The absence of nitrogen in the XPS spectra can be attributed to

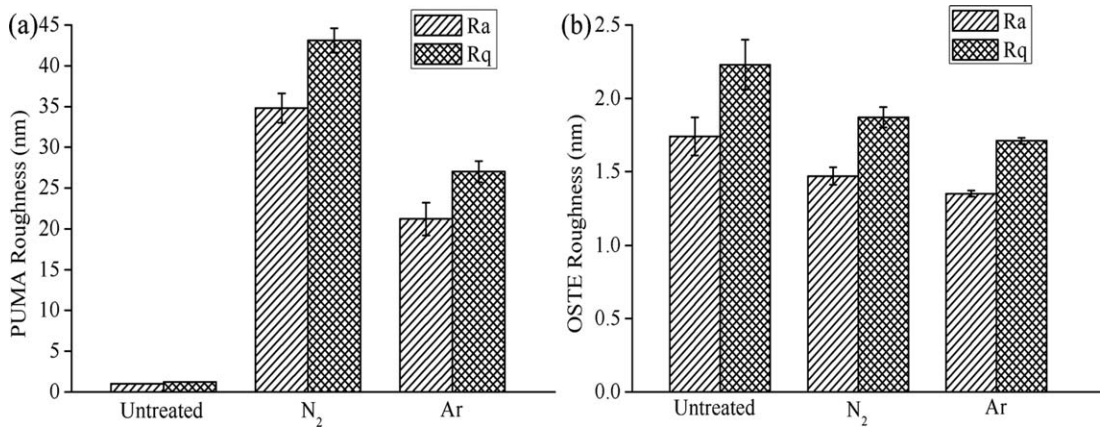

Figure 4. Average (Ra) and root mean square roughness (Rq) of untreated, Ar or N_2 plasma-treated (a) PUMA polymers and (b) OSTE-80 polymers after 10 sccm, 20 W, 60 seconds and 30 seconds, respectively. Error bars represent means ± SD for $n = 3$, $^*P < 0.05$.

the low concentration of the nitrogen in the PUMA polymer though polyurethane, per se, showed a typical concentration of 4% for nitrogen.[34] Our analysis was complicated by the proprietary mixture of PUMA prepolymers procured from Polydiam, i.e., the actual amide percentage could be minuscule in Polydiam PUMA. Another possibility for this absence of nitrogen in the XPS analysis is the migration of this polar nitrogen moieties into the PUMA polymer beyond the XPS analysis depth of 10 nm because of the interfacial enthalpy and entropy of these polar groups.[15] However, such typical migration occurred over the time span of several days or weeks which will be discussed next section, and our XPS analysis were carried out within one day of plasma treatment.

As expected, the nitrogen content of PUMA polymers increased to 7.0% and 2.2% after N_2 and Ar plasma treatment, respectively (Table I). During N_2 plasma treatment of PUMA, different reactive species such as N^+ and N^{2+} formed in the chamber, and these ions incorporated and enriched the PUMA polymers.

On the other hand, Ar plasma treatment was not expected to incorporate any nitrogen moieties onto PUMA or OSTE-80 polymers because of the inert Ar monomers used in plasma treatment.[35] Under certain high discharge power, nitrogen moieties were reported on the Ar plasma-treated Nafion[18] or polyethylene.[36,37] While Bae *et al.* did not discuss the origin of this nitrogen,[18] others attributed the nitrogen moieties to the residual reactor atmosphere, post-treatment storage, desorption from the wall and residual nitrogen from the processing gas.[36,37] Hollaender *et al.* further claimed that these residual nitrogen oxidized to nitric oxide which recombined with radicals on the polyethylene.[37] Here, we speculated that similar mechanism introduced the nitrogen moieties onto the PUMA polymers.

Table I. Elemental Composition and Atomic Ratios of PUMA Polymers before and after N_2 and Ar Plasma Treatment

	Atomic percentage (%)			Atomic ratio	
	C1s	N1s	O1s	N1s/C1s	O1s/C1s
Untreated	74.5	0	25.5	0	0.34
N_2 Plasma	76.4	7.0	16.6	0.09	0.22
Ar Plasma	78.1	2.2	19.7	0.03	0.25

Figure 5(a) shows the deconvolution of the C1s peak of PUMA polymers into five components: the aliphatic/aromatic hydrocarbon peak (C—C, C—H) at 285.0 eV, the amine peak (C—N) at 286.0, the ether peak (C—O—C) at 286.5 eV, the carbonyl peak (C=O) at 288.0 eV, and also the urethane peak (N—COO) at 289.0 eV.[34,38,39] The ether and urethane peaks represented the soft and hard segments of the PUMA polymers, respectively.[20,38]

The component C1s spectra of PUMA polymers showed that the main component of the PUMA polymers was the ether bonds (C—O—C). When the PUMA polymers were plasma treated with N_2 plasma, the concentration of these ether groups was reduced from 41.0% to 9.9% (Table II). A similar reduction in ether groups occurred when the PUMA polymers were Ar plasma treated, as shown on Figure 5(a) and Table II. The reduction of the ether group implied the removal of the soft segments while the hard segment, i.e., urethane group (N—COO), retained during the Ar and N_2 plasma treatment of the PUMA polymers.

Based on Figure 5(b), the N1s spectra of Ar or N_2 plasma-treated PUMA polymers can be deconvoluted to the following functional groups with their respective binding energies: amine (C—N) at 398.9–399.1 eV, imine (C=N) at 400.1–400.2 eV, and amide groups (N—C=O) at 401.0–401.2 Ev, respectively.[21,40] The atomic percentage for these N-containing functional groups are reported in Table II. As mentioned earlier, the XPS analysis of the untreated PUMA polymer did not show any nitrogen despite the presence of amide in its molecular structure. A high percentage of the N1s spectra was attributed to imine groups which were commonly found in such plasma treatment process while the amines oxidized to amide groups as part of the ageing process of the plasma-treated PUMA polymers.[41] These nitrogen moieties as well as the carboxyl groups from the hydrocarbon increased the hydrophilicity and reduced the WCA of the plasma-treated PUMA.

Ar and N_2 plasma-treatment on OSTE-80 polymers. As shown in Figure 1(b), one of the OSTE-80 prepolymers is

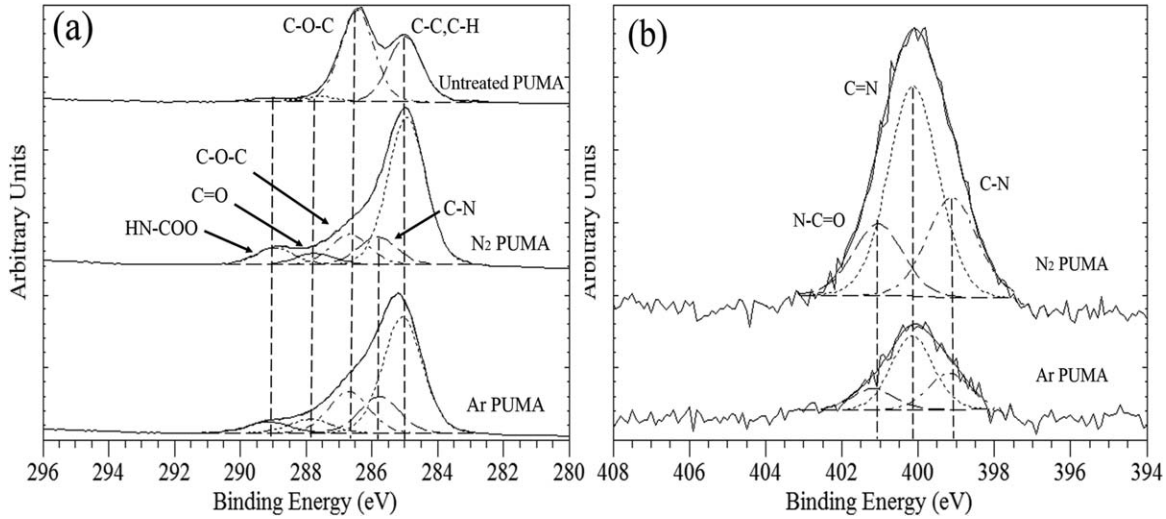

Figure 5. Component-fitted (a) C1s and (b) N1s peaks of PUMA polymers before and after plasma treatments with N_2 and Ar for 10 sccm, 20W, and 60 seconds, respectively. Note: XPS analysis of untreated PUMA polymer did not show any nitrogen.

Table II. Component-Fitted C1s and N1s Spectra of PUMA Polymers before and after N_2 and Ar Plasma Treatment

	C1s (at %) [34,38,39]					N1s (at %) [21,40]		
BE (eV)	C—C 285.0	C—N 286.0	C—O—C 286.5	C=O 288.0	N—COO O—C=O 289.0	C—N 399.1	C=N 400.1	N—C=O 401.1
Untreated	29.3	—	41.0	2.4	1.8	—	—	—
N_2 Plasma	48.4	9.1	9.9	3.7	5.3	1.8	3.9	1.3
Ar Plasma	41.5	13.0	14.8	4.9	3.9	0.6	1.2	0.4

1,3,5-triallyl-1,3,5-triazine-2,4,6(1H,3H,5H)-trione and this prepolymer contains the nitrogen to form the amide groups. This nitrogen was detected in the XPS survey scan of the untreated OSTE-80 polymers, and after plasma treatment with Ar and N_2 (Table III). Ar and N_2 plasma treatment doubled the nitrogen content of OSTE-80 polymers to 6–7 at %; the N/C ratios increase from 0.05 to 0.10 for the plasma-treated OSTE-80 polymers. There were no visible changes in

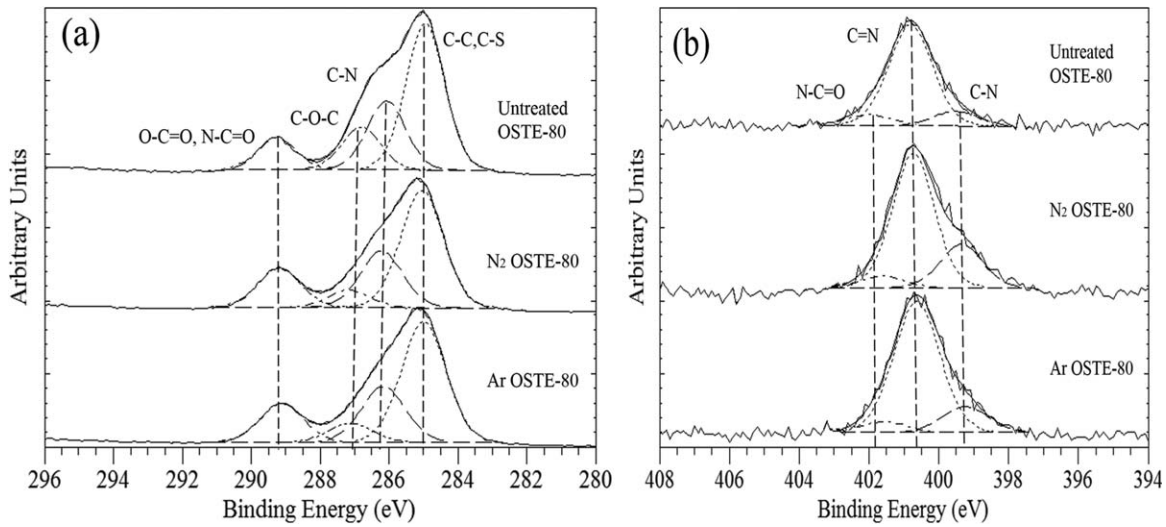

Figure 6. Component-fitted XPS spectra of (a) C1s and (b) N1s peaks of OSTE-80 polymers before and after plasma treatment with N_2 and Ar at 10 sccm, 20 W, 30 seconds, respectively.

Table III. Elemental Composition and Atomic Ratios of OSTE-80 Polym1ers before and after Ar and N_2 Plasma Treatment

	Atomic percentage (%)				Atomic ratio		
	C1s	N1s	O1s	S2p	N1s/C1s	O1s/C1s	S2p/C1s
Untreated	66.0	3.3	24.7	6.0	0.05	0.37	0.09
N_2 Plasma	63.7	6.2	24.4	5.7	0.10	0.38	0.09
Ar Plasma	65.7	6.7	23.0	4.6	0.10	0.35	0.07

the S/C and O/C ratios for the Ar and N_2 plasma-treated OSTE-80 polymers.

The four components and binding energies of the deconvoluted C1s spectra of the OSTE-80 polymer are shown in Figure 6(a) and tabulated in Table IV. While there was no significant difference in the percentage of C—N group between untreated and plasma-treated OSTE-80 polymer, those related to C—O—C and C—OH halved after Ar and N_2 plasma treatment. The lack of differences in the atomic percentage of C-N groups suggested the integrity of the prepolymer (i.e., 1,3,5-triallyl-1,3,5-triazine-2,4,6(1H,3H,5H)-trione) which contains this C-N groups during the Ar and N_2 plasma treatment.

In the case of C—O—C and C—OH groups which share the similar binding energy of 286.5 eV, there was no chemical derivatization to differentiate them but this percentage was likely to be referring to the C—O—C groups from one of the OSTE-80 prepolymers [i.e., pentaerythrithiol tetrakis (3-mercaptopropionate)] which remained intact after UV-curing. The reduction in the percentage of C—O—C groups suggested that OSTE-80 polymers suffered from bond scission within this ether group after Ar or N_2 plasma treatment. This component at 286.5eV could not have been C—OH groups because postplasma oxidation would increase the percentage of C-OH groups in the N_2 and Ar plasma-treated OSTE-80 polymer.[15]

Table IV also shows some marginal increase in functional groups related to O—C=O and N—C=O after plasma treatment with Ar or N_2; such increase implied the presence of oxidized carboxyl moieties or the amide groups from the oxidation of amine on the Ar or N_2 plasma-treated OSTE-80 polymers.

Based on Figure 6(b) and Table IV, the main components of the N1s spectra of the OSTE-80 polymers are amine (C—N), imine (C=N), and amide (N—C=O). The binding energies of the imine and amide groups for OSTE-80 polymers were higher than those used to component-fit the N1s of PUMA polymers because of the higher percentage of the electro-negative oxygen moieties within the plasma-treated OSTE-80 polymers. Oxygen atoms were known to draw the electrons from the nitrogen resulting in higher binding energies for their nitrogen moieties but still within the reported binding energies for imine and amide.[42,43]

As mentioned earlier in Table III, there was only a slight reduction in sulfur content after Ar or N_2 plasma treatment on OSTE-80 polymers which suggested minimum etching of the C—S or S—H bonds within the OSTE-80 polymers. Based on the component-fitted S2p spectra provided in the supplementary data, the oxidation state of the sulfur moieties did not change during the Ar or N_2 plasma treatment. This absence of change in oxidation states ensured that OSTE-80 polymers can be bonded to produce the biochip.[6]

Ageing Properties of PUMA and OSTE-80 Polymers after Plasma Treatment

Plasma modified polymers suffered from ageing during storage after their plasma treatment or plasma polymerization. In general, ageing is characterized by postplasma oxidation, surface adaptation and volatilization of heteroatom moieties from the plasma modification process.[15] Postplasma oxidation introduces polar groups like carboxyl, amine, imine, and amide onto the surfaces while surface adaptation restructures these polar groups into the bulk polymers driven by the entropy and interfacial enthalpies of these polar groups.[15] Such ageing properties are often characterized by multiple complementary instruments such as WCA, AFM, and XPS. WCA detects any changes in polarities in the outermost nanometers of the polymer while XPS probes any chemical changes within top 10 nm of the substrate.

Ageing Properties of PUMA Polymers after Ar and N_2 Plasma Treatment. Based on Figure 7, the WCA of the Ar and N_2 plasma-treated PUMA polymers increase from 50° to different stable values within the first 10 hours of ageing regardless of the storage mediums. Continuous ageing in these environments did not revert the WCA back to those of untreated PUMA polymers; this partial recovery is similar to those reported earlier for Ar plasma-treated FEP.[44] The partial recovery of Ar or N_2

Table IV. Component-Fitted C1s and N1s Spectra of OSTE-80 Polymers before and after N_2 and Ar Plasma Treatment

	C1s (at %)[39]				N1s (at %)[42,43]		
BE (eV)	C—C, C—S (285.0)	C—N (286.0)	C—O—C (286.5)	O—C=O, N—C=O (289.0)	C—N (399.3)	C=N (400.7)	N—C=O (402.0)
Untreated	33.5	15.7	9.7	7.1	0.4	2.6	0.3
N_2 Plasma	32.5	15.6	4.8	10.8	1.4	4.4	0.4
Ar Plasma	33.8	15.7	5.4	10.8	1.1	5.2	0.4

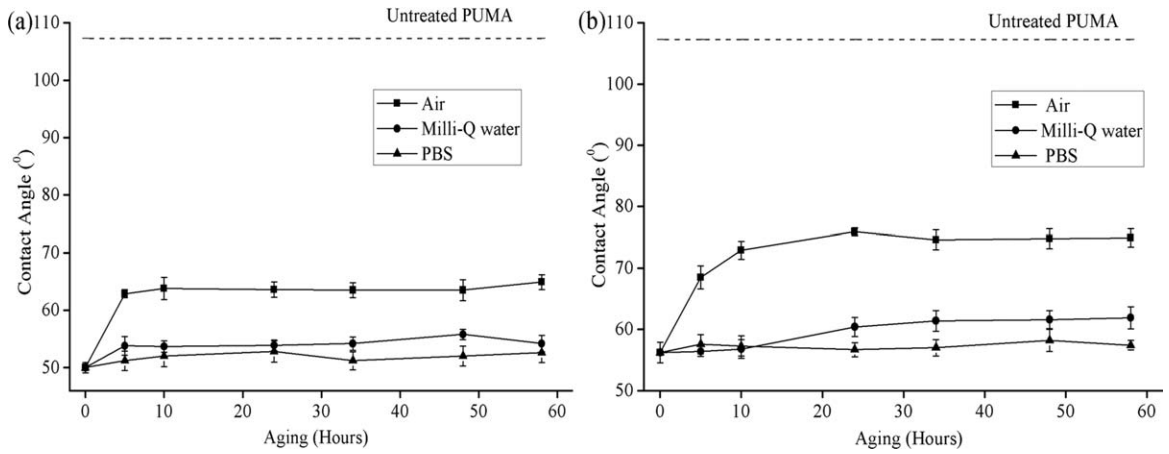

Figure 7. Water contact angle of the (a) N_2 and (b) Ar plasma-treated PUMA polymers after ageing in air, Milli-Q water, and PBS for different durations. The plasma treatment conditions for N_2 and Ar are 60 seconds, 10 sccm and 20 W.

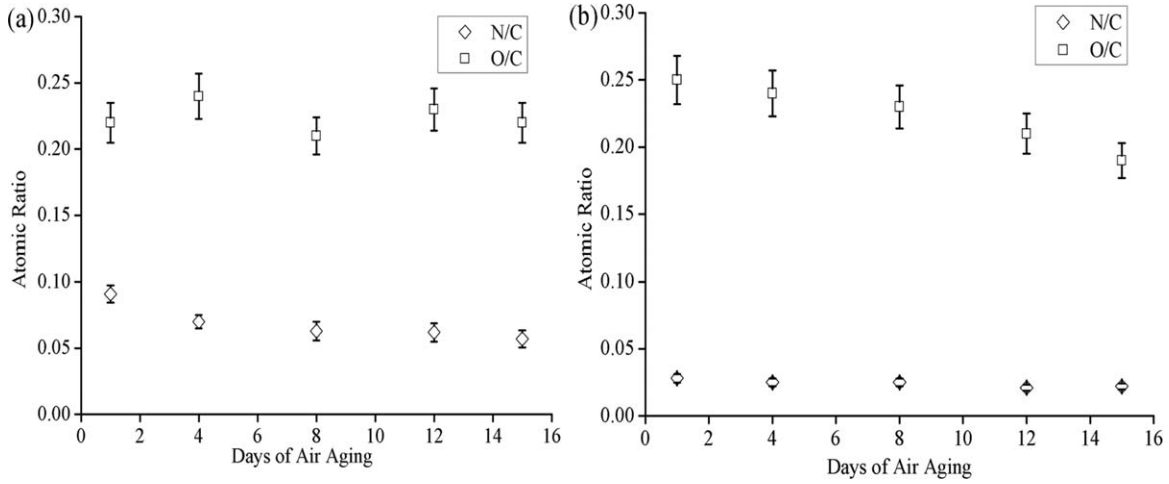

Figure 8. XPS atomic ratios of the plasma-treated PUMA polymers with (a) N_2 and (b) Ar and after 15 days of air-ageing. The process conditions for the N_2 and Ar plasma are 60 seconds, 10 sccm, and 20 W.

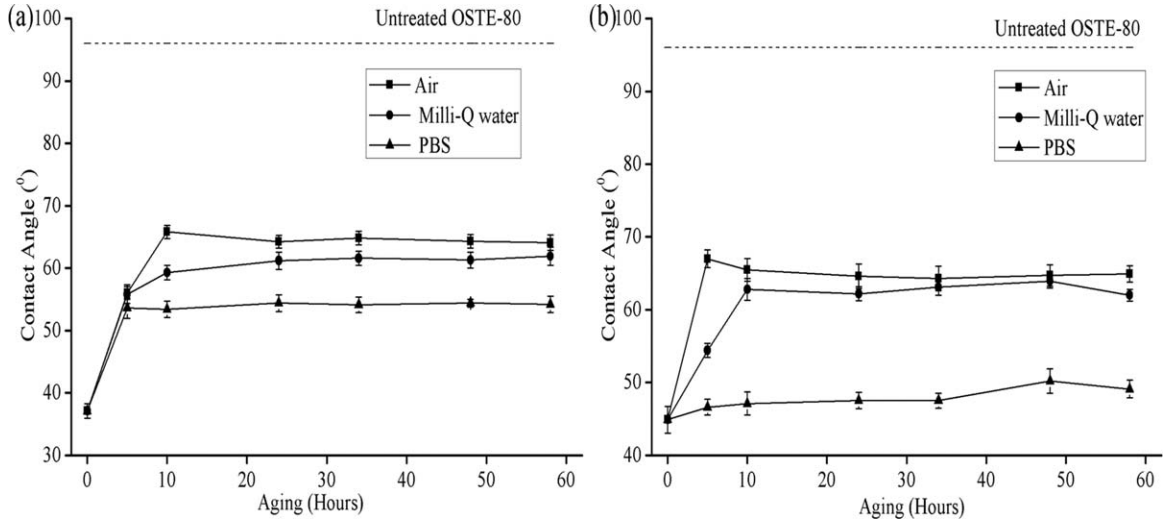

Figure 9. Water contact angle of the (a) N_2 and (b) Ar plasma-treated OSTE-80 polymers after ageing in air, Milli-Q water and PBS for different durations. The plasma treatment conditions for N_2 and Ar are 30 seconds, 10 sccm, and 20 W.

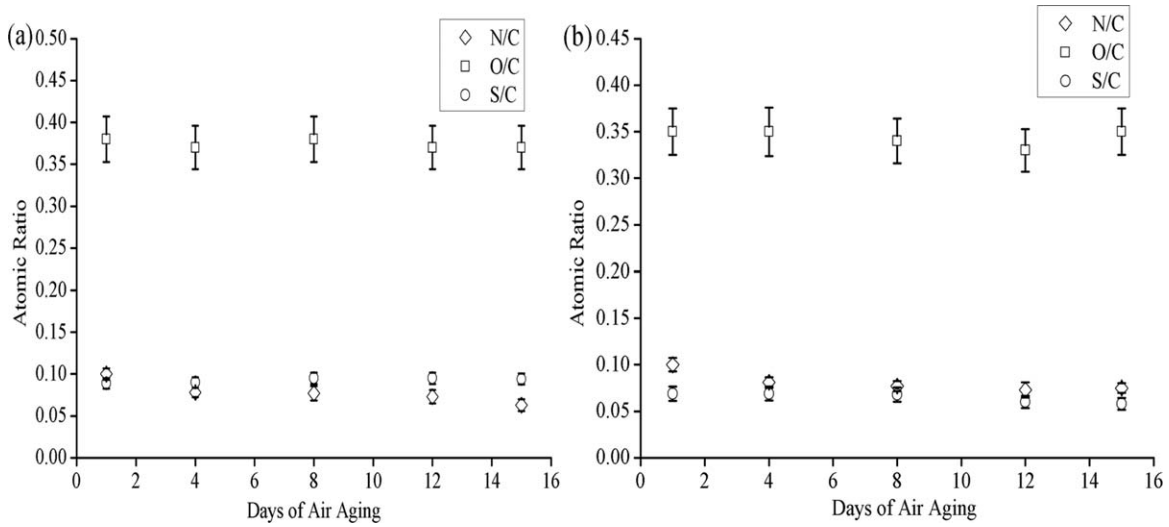

Figure 10. XPS atomic ratios of the OSTE-80 polymers plasma-treated with (a) N_2 and (b) Ar plasma for 15 days of air-ageing. The plasma process conditions for N_2 and Ar are 30 seconds, 10 sccm, and 20 W applied.

plasma-treated PUMA polymers suggested there are mobile and immobile polar groups which responded differently to the different ageing environments.[44]

The hydrophobic recovery of the plasma-treated PUMA polymers in Milli-Q water and PBS was less than those aged under ambient air atmosphere (Figure 7). This reduction was expected because of the preferential migration of those polar group on the plasma-treated PUMA to "bond" with the water molecules at the interface of the liquid media.[45,46] This migration has been attributed to the short range forces induced by the higher dielectric constants of the liquid medium ($\varepsilon > 80$) compared to the typical dielectric constants of polymers ($10 > \varepsilon > 2$).[45] The differences in hydrophobic recovery for Ar and N_2 plasma-treated PUMA polymers in Milli-Q and PBS would not be significant because the dielectric constant of Milli-Q was only slightly higher than PBS.[47]

Although the WCA of the N_2 plasma-treated PUMA polymer showed stable value within 10 hours of ageing, the N/C ratios of XPS [Figure 8(a)] continue to reduce for the first eight days of ageing. Since WCA and XPS probe different depth of analysis, we can deduce that the initial increase in WCA analysis coincided with the migration of the polar nitrogen moieties into the bulk PUMA polymer and subsequent stabilization amongst themselves.[44] This stabilization was supported by the lack of changes in WCA and the O/C ratios during the 15 days of air-ageing. Continuous oxidation increases the hydrophilicity of a N_2 plasma-treated substrates and reduces their WCAs, but Figure 8 shows the subsequent reduction in N/C ratios between 10 hours and 8 days of air ageing. This reduction was likely to be related to the volatilization of different nitrogen groups from the N_2 plasma-treated PUMA polymer though such hypothesis needs to be confirmed by angle-resolved XPS.

The O/C ratio of the Ar plasma-treated PUMA polymer, shown on Figure 8(b), reduced continuously for the 15 days of air ageing, while the WCA of Ar plasma-treated PUMA polymers achieved stability within 10 hours of air ageing. Within the first

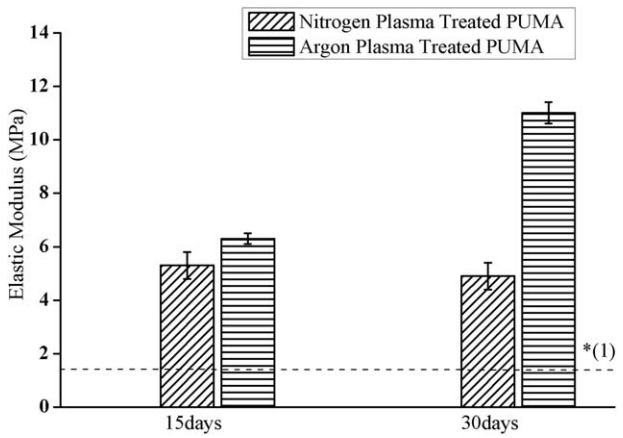

Figure 11. N_2 and Ar plasma treatment increased the elastic modulus of the PUMA polymer after 15 days and 30 days of ageing in air. Error bars represent means ± SD for $n = 3$, $^*P < 0.05$. *(1) refers to the elastic modulus of an untreated PUMA polymer.

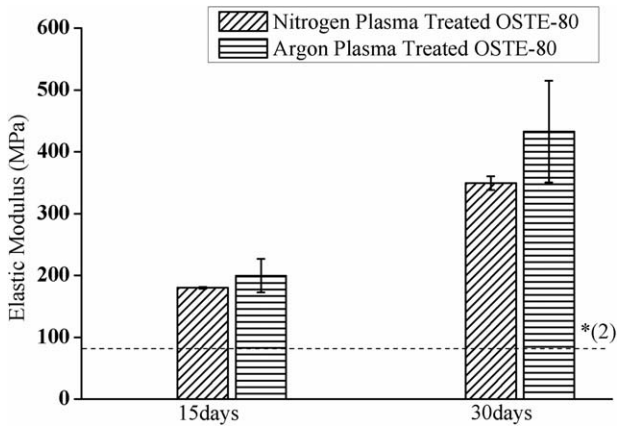

Figure 12. N_2 and Ar plasma treatment increased the elastic modulus of the OSTE-80 polymer after 15 and 30 days ageing in air. Error bars represent means ± SD for $n = 3$, $^*P < 0.05$. *(2) refers to the elastic modulus of an untreated OSTE-80 polymer.

Table V. Chemical and Physical Properties of PDMS, PUMA, and OSTE-80 Polymers before and after N_2, Ar and O_2 Plasma Treatments

Polymers before and after plasma treatments	Nitrogen composition of XPS (%)	Rq (nm)	WCA (°)		Elastic modulus (MPa)	
			Immediate	Air ageing	Immediate	Air ageing
PDMS	0	7.0[51]	110.0[22]	110[22]	1.5[52] - 3.4[53]	—
PDMS N_2	1.2[54]	8.0[51]	10.0[55]	78.4[55]	—	—
PDMS Ar	0[54]	13.0[51]	5.0[22]	85.0[22]	3.0[52]	—
PDMS O_2	0.9[56]	14.0[51]	41.0[56]	90.0[56]	56.0[53]	40.1[a53]
PUMA	0	1.2	107.3	107.3	1.2	1.2
PUMA N_2	7.0	43.1	50.0	64.9	—	5.3[b]
PUMA Ar	2.2	27.0	56.2	74.9	—	6.3[b]
OSTE-80	3.3	2.2	96.0	96.0	73.0	73.0
OSTE-80 N_2	6.2	1.9	37.1	64.1	—	180.2[b]
OSTE-80 Ar	6.7	1.7	44.9	64.9	—	199.6[b]

[a] Aged for 7 days.
[b] Aged for 15 days.

60 hours of air ageing, the lack of change in WCA coincided with the insignificant change in the ratio of O/C measured on the first and fourth days of air ageing but subsequent air ageing reduced the O/C ratios. Typically, postplasma oxidation increased the O/C ratios, but hydrophobic recover could also bury these polar groups into the bulk polymers beyond the XPS analysis depth, to reduce the O/C ratios. Alternatively, the oxidized nitrogen oligomers on the Ar plasma-treated PUMA polymer could volatize to the atmosphere or solubilize during the aqueous washing in the sample preparation step before XPS analysis. The second mechanism was unlikely to happen because the N/C ratios remained constant during the 15 days of air ageing.

Ageing Properties of OSTE-80 Polymers after Ar and N_2 Plasma Treatment. Figures 7 and 9 show a similar trend of WCA between the OSTE-80 and PUMA polymers after plasma treatment with Ar and N_2, respectively; the WCA of OSTE-80 polymers stabilized to different degrees within the first 10 hours of ageing. Unlike PUMA polymer, the WCA of Ar and N_2 plasma-treated OSTE-80 polymers showed the merging of WCA for the air and Milli-Q water after 20 and 60 hours of ageing, respectively, in spite of their big differences in dielectric strength. This difference can be attributed to the nature and quantity of the radicals created by the Ar or N_2 plasma treatment in the OSTE-80 polymers, but such hypothesis could only be confirmed by electron spin resonance spectroscopy, which was beyond the current scope of work.

The stability of the WCA, shown in Figure 9, is also reflected by the stability in the atomic ratios of the plasma-treated OSTE-80 polymer though both measurements refer to different time scales. The S/C and O/C ratios of OSTE-80 polymers maintained their respective ratios within 15 days of air-ageing after Ar and N_2 plasma treatment (Figure 10). The N/C ratios for the Ar and N_2 plasma-treated OSTE-80 polymers only reduced slightly within first four days of air ageing. This slight reduction could be attributed to the hydrophobic recovery which buried the nitrogen moieties into the OSTE-80 polymers or volatilization of these nitrogen moieties into the atmosphere during the ageing period. The stability of these N/C ratios maintained the hydrophilicity of these Ar or N_2 plasma-treated OSTE-80 polymers.

Elastic Modulus of PUMA and OSTE-80 Polymers after Ar and N_2 Plasma Treatment. Elastic modulus is measured during these ageing as a proxy for crosslinking density; a high elastic modulus implies a high crosslinking density which reduces the surface mobilities and migration of these polar groups into the bulk polymer. Figures 11 and 12 show the increase of elastic modulus of the PUMA and OSTE-80 polymers after plasma treatment. The elastic modulus of PUMA polymer was 1.2 MPa which agreed with those reported in the literature.[10] After N_2 plasma treatment, the elastic modulus of the PUMA polymer increased fourfold to 5.3 and 4.9 MPa after 15 and 30 days of air ageing, respectively. Ar plasma treatment resulted in a higher increase of elastic modulus for the PUMA polymer than N_2 plasma treatment because of the higher number of generated radicals which cross-linked amongst themselves to produce a stiff matrix. This mechanism of Ar plasma treatment is similar to the CASING (crosslinking by activated species of inert gas) technique used to create a highly cross-linked polymer reported elsewhere.[48]

Based on Figure 12, the elastic modulus of OSTE polymers increased from 73 MPa to 180 and 349 MPa after 15 and 30 days of air ageing after treated with N_2 plasma. Unlike PUMA, there was no significant difference in the elastic modulus of the OSTE-80 between the N_2 and Ar plasma after 15 or 30 days of air ageing ($^*P < 0.05$). This lack of difference could be attributed to the amorphous nature of OSTE-80.

When the plasma-treated PUMA and OSTE-80 polymers aged during storage or part of the processing steps in making

biochip, their increase in stiffness would maintain the microstructures to prevent buckling or deformation in the microfluidic chip.[11,49] Based on the elastic moduli in Figures 11 and 12, PUMA polymer is more suited for the valves and actuators of the lab-on-chip devices while OSTE-80 polymer is used for fabricating the body of the microfluidic devices.

Summary

The physical and chemical properties of PDMS, PUMA, and OSTE-80 polymers are summarized in Table V. Overall, plasma-treated PUMA and OSTE-80 polymers possess higher nitrogen composition, hydrophilicity, and stiffness as compared to properties of PDMS polymer reported in the public literature. After plasma treatment, PUMA and OSTE-80 polymers had various nitrogen-containing groups which can possibly be used for prototyping a biocompatible microfluidic device. In microfluidic applications, a hydrophilic surface of plasma-treated PUMA and OSTE-80 might help to improve the wettability of the aqueous solutions and reduces nucleation of air bubbles in the microchannels.[50] Furthermore, surface crosslinking of the plasma-treated PUMA and OSTE-80 resulted in high elastic modulus to maintain its microstructures when they are used as a mold to transfer the patterns onto a subsequent substrate. Therefore, plasma-treated PUMA and OSTE-80 polymers are potential candidates for replacing the PDMS in prototyping microfluidic devices.

CONCLUSIONS

In this article, N_2 and Ar plasma modified the PUMA and OSTE-80 polymers by inserting different nitrogen functional groups, such as amine, imine, and amide on the surfaces. The WCA of the plasma-treated OSTE-80 polymer increased and stabilized to different contact angles depending on the ageing medium within 10 hours of ageing. A similar trend was reported for the WCA of the plasma-treated PUMA polymer for the same period of ageing, but their XPS analysis showed different atomic ratios. During the 15 days of air ageing, the slight reduction of N/C ratios could be attributed to the hydrophobic recovery within the Ar or N_2 plasma-treated OSTE-80. A similar reduction occurred for the Ar or N_2 plasma-treated PUMA polymer. This reduction and subsequent stabilization of the N/C ratios after 8 days of air-ageing showed that these plasma modified OSTE-80 and PUMA polymers were stable and maintained their nitrogen moieties on their surfaces for subsequent bio-interfacial interactions. In terms of mechanical properties, Ar plasma generated more radicals within PUMA polymer than N_2 plasma, which subsequently cross-linked to a high elastic modulus during their 30 days of air ageing. Such differences were not reflected in the N_2 and Ar plasma treatment of OSTE-80 polymer which increased similarly by two folds and five folds during their 15 and 30 days of air ageing. Nevertheless, the increase of elastic modulus during air ageing presented an additional avenue to stiffen the structures of the plasma modified polymers.

ACKNOWLEDGMENTS

We would like to acknowledge the following grants for these works: Malaysia Ministry of Education Hi-Centre of Excellence MEMS for Artificial Kidney (AKU-95), Fundamental Research Grant Scheme (FRGS/2/2013/SG06/UKM/02/3) and Universiti Kebangsaan Malaysia Research University Grant (GUP/2015/039).

REFERENCES

1. Jang, K. J.; Mehr, A. P.; Hamilton, G. A.; McPartlin, L. A.; Chung, S.; Suh, K. Y.; Ingber, D. E. *Integr. Biol.* **2013**, *5*, 1119.
2. Kurkuri, M. D.; Al-Ejeh, F.; Shi, J. Y.; Palms, D.; Prestidge, C.; Griesser, H. J.; Brown, M. P.; Thierry, B. *J. Mater. Chem.* **2011**, *21*, 8841.
3. van Midwoud, P. M.; Janse, A.; Merema, M. T.; Groothuis, G. M.; Verpoorte, E. *Anal. Chem.* **2012**, *84*, 3938.
4. Regehr, K. J.; Domenech, M.; Koepsel, J. T.; Carver, K. C.; Ellison-Zelski, S. J.; Murphy, W. L.; Schuler, L. A.; Alarid, E. T.; Beebe, D. *J. Lab Chip* **2009**, *9*, 2132.
5. Jin, Y. H.; Cho, Y. H.; Schmidt, L. E.; Leterrier, Y.; Månson, J. A. E. *J. Micromech. Microeng.* **2007**, *17*, 1147.
6. Carlborg, C. F.; Haraldsson, T.; Öberg, K.; Malkoch, M.; van der Wijngaart, W. *Lab Chip* **2011**, *11*, 3136.
7. Kim, J.; Chaudhury, M. K.; Owen, M. J. *J. Colloid Interface Sci* **2000**, *226*, 231.
8. Alvankarian, J.; Bahadorimehr, A.; Majlis, B. Y. *Biomicrofluidics* **2013**, *7*, 014102.
9. Kuo, J. S.; Ng, L.; Yen, G. S.; Lorenz, R. M.; Schiro, P. G.; Edgar, J. S.; Zhao, Y.; Lim, D. S.; Allen, P. B.; Jeffries, G. D. *Lab Chip* **2009**, *9*, 870.
10. Alvankarian, J.; Majlis, B. Y. *J. Micromech. Microeng.* **2012**, *22*, 035006.
11. Kuo, J. S.; Zhao, Y.; Ng, L.; Yen, G. S.; Lorenz, R. M.; Lim, D. S.; Chiu, D. T. *Lab Chip* **2009**, *9*, 1951.
12. Saharil, F.; Carlborg, C. F.; Haraldsson, T.; Van Der Wijngaart, W. *Lab Chip* **2012**, *12*, 3032.
13. Carlborg, C. F.; Saharil, F.; Haraldsson, T.; Wijngaart, W. v. d. 15th International Conference on Miniaturized Systems for Chemistry and Life Sciences 2011, MicroTAS 2011; Seattle, WA; United States; 2–6 October, **2011**, p 1143.
14. Errando-Herranz, C.; Vastesson, A.; Zelenina, M.; Pardon, G.; Bergström, G.; Wijngaart, W. v. d.; Haraldsson, T.; Brismar, H.; Gylfason, K. B. The 17th International Conference on Miniaturized Systems for Chemistry and Life Sciences (MicroTAS 2013), Freiburg, 27–31 October, **2013**.
15. Siow, K. S.; Britcher, L.; Kumar, S.; Griesser, H. J. *Plasma Processes Polym.* **2006**, *3*, 392.
16. Siow, K. S.; Kumar, S.; Griesser, H. *J. Plasma Processes Polym.* **2015**, *12*, 8.
17. Cvelbar, U.; Junkar, I.; Modic, M. *Jpn. J. Appl. Phys.* **2011**, *50*, 08JF02.
18. Bae, B.; Kim, D.; Kim, H. J.; Lim, T. H.; Oh, I. H.; Ha, H. Y. *J. Phys. Chem. B* **2006**, *110*, 4240.
19. Vesel, A.; Junkar, I.; Cvelbar, U.; Kovac, J.; Mozetic, M. *Surf. Interface Anal.* **2008**, *40*, 1444.
20. Alves, P.; Pinto, S.; de Sousa, H. C.; Gil, M. H. *J. Appl. Polym. Sci.* **2011**, *122*, 2302.

21. Roy, S.; Yue, C. Y. *Plasma Processes Polym.* **2011**, *8*, 432.
22. Pinto, S.; Alves, P.; Matos, C.; Santos, A.; Rodrigues, L.; Teixeira, J.; Gil, M. *Colloids Surf. B Biointerfaces* **2010**, *81*, 20.
23. Pardon, G.; Haraldsson, T.; van der Wijngaart, W. 2014 IEEE 27th International Conference on Micro Electro Mechanical Systems (MEMS), **2014**, p 96.
24. Siow, K. S.; Britcher, L.; Kumar, S.; Griesser, H. *J. Plasma Processes Polym.* **2014**, *11*, 133.
25. Magonov, S. N.; Reneker, D. H. *Annu. Rev. Mater. Sci.* **1997**, *27*, 175.
26. Siow, K. S.; Britcher, L.; Kumar, S.; Griesser, H. *J. Plasma Processes Polym.* **2009**, *6*, 583.
27. Vuillequez, A.; Moreau, J.; Garda, M.; Youssef, B.; Saiter, J. *J. Polym. Res.* **2008**, *15*, 89.
28. Lin-Vien, D.; Colthup, N. B.; Fateley, W. G.; Grasselli, J. G. The Handbook of Infrared and Raman Characteristic Frequencies of Organic Molecules; Elsevier, **1991**.
29. Sikanen, T. M.; Lafleur, J. P.; Moilanen, M. E.; Zhuang, G.; Jensen, T. G.; Kutter, J. P. *J. Micromech. Microeng.* **2013**, *23*, 037002.
30. Sanchis, M.; Calvo, O.; Fenollar, O.; Garcia, D.; Balart, R. *Polym. Test.* **2008**, *27*, 75.
31. Inagaki, N.; Narushim, K.; Tuchida, N.; Miyazaki, K. *J. Polym. Sci. Part B: Polym. Phys.* **2004**, *42*, 3727.
32. Jacobs, T.; De Geyter, N.; Morent, R.; Van Vlierberghe, S.; Dubruel, P.; Leys, C. *Surf. Coat. Technol.* **2011**, *205*, S511.
33. Anselme, K.; Bigerelle, M. *Int. Mater. Rev.* **2011**, *56*, 243.
34. Sanchis, M. R.; Calvo, O.; Fenollar, O.; Garcia, D.; Balart, R. *Plasma Processes Polym.* **2007**, *4*, S1091.
35. Gerenser, L. *J. Adhes. Sci. Technol.* **1987**, *1*, 303.
36. Švorčík, V.; Kotál, V.; Siegel, J.; Sajdl, P.; Macková, A.; Hnatowicz, V. *Polym. Degrad. Stab.* **2007**, *92*, 1645.
37. Holländer, A.; Kröpke, S. *Surf. Coat. Technol.* **2011**, *205*, S480.
38. Wilson, D.; Rhodes, N.; Williams, R. *Biomaterials* **2003**, *24*, 5069.
39. Vickerman, J. C.; Gilmore, I. S. Surface Analysis: The Principal Techniques; Wiley Online Library, **2009**.
40. Shahidzadeh-Ahmadi, N.; Arefi-Khonsari, F.; Amouroux, J. *J. Mater. Chem.* **1995**, *5*, 229.
41. Gengenbach, T. R.; Chatelier, R. C.; Griesser, H. *J. Surf. Interface Anal.* **1996**, *24*, 271.
42. Gancarz, I.; Poźniak, G.; Bryjak, M.; Tylus, W. *Eur. Polym. J.* **2002**, *38*, 1937.
43. Mutel, B.; Grimblot, J.; Dessaux, O.; Goudmand, P. *Surf. Interface Anal.* **2000**, *30*, 401.
44. Griesser, H. J.; Da, Y.; Hughes, A. E.; Gengenbach, T. R.; Mau, A. W. *Langmuir* **1991**, *7*, 2484.
45. Chen, I. J.; Lindner, E. *Langmuir* **2007**, *23*, 3118.
46. Ma, K.; Rivera, J.; Hirasaki, G. J.; Biswal, S. L. *J. Colloid Interface Sci* **2011**, *363*, 371.
47. Chaplin, M. **2015**. http://www1.lsbu.ac.uk/water/microwave_water.html. (Accessed 28th March 2016).
48. Schonhorn, H.; Hansen, R. *J. Appl. Polym. Sci.* **1967**, *11*, 1461.
49. Sollier, E.; Murray, C.; Maoddi, P.; Di Carlo, D. *Lab Chip* **2011**, *11*, 3752.
50. Martin, B. D.; Brandow, S. L.; Dressick, W. J.; Schull, T. L. *Langmuir* **2000**, *16*, 9944.
51. Williams, R.; Wilson, D.; Rhodes, N. *Biomaterials* **2004**, *25*, 4659.
52. Feinberg, A.; Brennan, A. Abstracts of Papers of the American Chemical Society; **2003**, *225*, U711.
53. Yang, Y.; Kulangara, K.; Lam, R. T.; Dharmawan, R.; Leong, K. W. *ACS Nano* **2012**, *6*, 8591.
54. Owen, M. J.; Smith, P. J. *J. Adhes. Sci. Technol.* **1994**, *8*, 1063.
55. Yang, C.; Yuan, Y. J. *Appl. Surf. Sci.* **2016**, *364*, 815.
56. Kaczorowski, W.; Szymanski, W.; Batory, D.; Niedzielski, P. *J. Appl. Polym. Sci.* **2015**, *132*, DOI: 10.1002/app.41635.